Haploinsufficiency of *Sox9* results in defective cartilage primordia and premature skeletal mineralization

Weimin Bi, Wendong Huang, Deanne J. Whitworth, Jian Min Deng, Zhaoping Zhang, Richard R. Behringer, and Benoit de Crombrugghe*

Department of Molecular Genetics and Graduate Program in Genes and Development, M. D. Anderson Cancer Center, University of Texas, Houston, TX 77030

Edited by Darwin J. Prockop, Tulane University, New Orleans, LA, and approved March 30, 2001 (received for review February 23, 2001)

In humans, *SOX9* heterozygous mutations cause the severe skeletal dysmorphology syndrome campomelic dysplasia. Except for clinical descriptions, little is known about the pathogenesis of this disease. We have generated heterozygous *Sox9* mutant mice that phenocopy most of the skeletal abnormalities of this syndrome. The *Sox9*$^{+/-}$ mice died perinatally with cleft palate, as well as hypoplasia and bending of many skeletal structures derived from cartilage precursors. In embryonic day (E)14.5 heterozygous embryos, bending of radius, ulna, and tibia cartilages was already prominent. In E12.5 heterozygotes, all skeletal elements visualized by using Alcian blue were smaller. In addition, the overall levels of *Col2a1* RNA at E10.5 and E12.5 were lower than in wild-type embryos. We propose that the skeletal abnormalities observed at later embryonic stages were caused by delayed or defective precartilaginous condensations. Furthermore, in E18.5 embryos and in newborn heterozygotes, premature mineralization occurred in many bones, including vertebrae and some craniofacial bones. Because *Sox9* is not expressed in the mineralized portion of the growth plate, this premature mineralization is very likely the consequence of allele insufficiency existing in cells of the growth plate that express *Sox9*. Because the hypertrophic zone of the heterozygous *Sox9* mutants was larger than that of wild-type mice, we propose that *Sox9* also has a role in regulating the transition to hypertrophic chondrocytes in the growth plate. Despite the severe hypoplasia of cartilages, the overall organization and cellular composition of the growth plate were otherwise normal. Our results suggest the hypothesis that two critical steps of the chondrocyte differentiation pathway are sensitive to *Sox9* dosage. First, an early step presumably at the stage of mesenchymal condensation of cartilage primordia, and second, a later step preceding the transition of chondrocytes into hypertrophic chondrocytes.

The differentiation of chondrocytes from mesenchymal cells occurs along a multistep pathway, during which committed mesenchymal cells first aggregate together to form precartilaginous condensations that prefigure the overall shape of future bones. Then expression of cartilage-specific proteins is initiated, and the cells become surrounded by abundant extracellular matrix (1). In the growth plate of endochondral bones, chondrocytes become flattened and undergo a unidirectional proliferation that is primarily responsible for the longitudinal growth of bones. After these cells stop proliferating, they change their genetic program and become hypertrophic. The extracellular matrix surrounding the hypertrophic chondrocytes that are closest to the metaphyses become mineralized and the cells undergo apoptosis, leaving behind a calcified cartilaginous matrix that is degraded subsequently and replaced by bone matrix (2).

Recent studies have identified SOX9 as an essential transcription factor in chondrogenesis (3). In the absence of *Sox9*, there is a complete block in chondrocyte differentiation, and the block occurs at the stage of mesenchymal condensations. SOX9 contains an SRY-related hydroxymethyl glutaryl (HMG) box DNA-binding domain and a transactivation domain rich in proline and glutamine. During mouse embryonic development, *Sox9* is expressed prominently in all chondrogenic precursor cells and in chondrocytes throughout the deposition of cartilage-specific matrix (4), but the expression of *Sox9* is switched completely off in hypertrophic chondrocytes (5). In addition to skeletal elements, *Sox9* also is expressed in developing gonads, heart, kidney, central nervous system, and pancreas (6, 7).

It has been suggested that the dosage of *SOX9* is critical for its normal function in humans. Mutations in a single allele of *SOX9* cause a severe skeletal malformation syndrome called campomelic dysplasia (CD; refs. 4, 6, and 8). In this disease, in which most skeletal elements derived from cartilage are affected, the characteristic clinical features are bowing and angulation of the tibiae and femura, hypoplastic scapulae, a missing pair of ribs, cleft palate, and micrognathia (9, 10). Nonskeletal abnormalities such as the absence of olfactory bulbs, dilatation of cerebral ventricles, and a variety of cardiac and renal defects also have been reported. In addition, about three-fourths of XY individuals develop as phenotypic females or intersexes (10).

Except for clinical descriptions of the disease, little is known about its pathogenesis. To better understand the human disease we generated heterozygous *Sox9* mutant mice. These mice die shortly after birth and display bending of long bones and hypoplasia of a variety of skeletal elements that strongly resemble those in patients with CD. Analysis of the course of the skeletal defects during embryonic development indicated that the cartilage primordia were malformed. Furthermore, premature mineralization was observed in a series of bones. Our results indicate that *Sox9* haploinsufficiency is manifested at two critical steps in the chondrocyte differentiation pathway—first, at an early step when cartilage primordia are formed and second, at a step preceding hypertrophic chondrocyte maturation.

Materials and Methods

Generation and Genotyping of the *Sox9* Mutant Mice. Embryonic stem cell lines containing mutations in one of the *Sox9* alleles were injected into blastocysts isolated from C57B6 mice that were reimplanted into the uteri of pseudopregnant CD-1 mice. Six male chimeras from two independent cell lines yielded germline transmission. The degree of chimerism of the founder mice varied from 70% to 95% based on agouti coat color. The heterozygotes were identified by Southern blot analysis and

This paper was submitted directly (Track II) to the PNAS office.

Abbreviations: E*n*, embryonic day *n*; CD, campomelic dysplasia; ES, embryonic stem.

*To whom reprint requests should be addressed at: Department of Molecular Genetics, 1515 Holcombe Boulevard, M. D. Anderson Cancer Center, University of Texas, Houston, TX 77030. E-mail: bdecromb@mdanderson.org.

The publication costs of this article were defrayed in part by page charge payment. This article must therefore be hereby marked "*advertisement*" in accordance with 18 U.S.C. §1734 solely to indicate this fact.

 www.pnas.org/cgi/doi/10.1073/pnas.111092198

β-galactosidase analysis. For Southern blot analysis, tail DNA was digested with *Eco*RI and hybridized with a 3′ external probe, as described (3).

Yolk sac-derived genomic DNA from embryos at E15.5 or earlier stages were genotyped by PCR. Primers specific for the *Sox9* wild-type allele were located inside the deleted region (sense primer, 5′-TGAATCTCCTGGACCCCTTC-3′ and antisense primer, 5′-TGCTGGAGCCGTTGACGCG-3′). Primers specific for the mutant allele were inside the *neomycin* gene (sense primer, 5′-GCCCTGAATGAACTGCAGGACG-3′ and antisense primer, 5′-CACGGGTAGCCAACGCTATGTC-3′). The reaction condition is 30 sec at 94°C, 1 min at 60°C, and 1 min at 72°C for 35 cycles.

Skeletal Analysis. Embryos at E14.5, E15.5, and E18.5 were dissected in PBS, and neonates were killed by using dry ice. The neonates then were skinned, eviscerated, and fixed in 95% ethanol. Skeletal preparation was performed as described (11). Alcian blue staining of cartilaginous tissue in E12.5 and E14.5 embryos was done according to a modification of the chicken embryo procedure (12).

Histological Analysis, *in Situ* Hybridization, and Immunohistochemical Analysis. Embryos were fixed in 4% formaldehyde, dehydrated with increasing ethanol concentration, and embedded in paraffin. Serial sections of 7 μm were stained with hematoxylin and eosin or Alcian blue. 5-bromo-4-chloro-3-indolyl β-D-galactoside (X-Gal) staining and radioactive RNA *in situ* hybridization were performed on sections as described (3). The *Col10a1* probe is a 550-bp *Bam*HI and *Hin*dIII fragment of mouse type X collagen cDNA.

Northern and Western Analyses. Primary chondrocytes were isolated from mouse rib cartilages as described (13). Briefly, ribs were dissected in PBS and digested with collagenase B. The isolated chondrocytes were used directly for RNA and cell lysates. Total RNA was prepared by RNeasy miniprep kit (Qiagen, Chatsworth, CA). The *Sox9* probe is a 300-bp fragment corresponding to the deleted region, and the *Col2a1* probe is a 405-bp *Hae*III and *Dra*I fragment from the exon corresponding to the 3′ untranslated sequence of *Col2a1* RNA (14). The same membrane was hybridized subsequently with *Sox9*, *Col2a1*, and *GAPDH* probes by stripping and rehybridization. Western analysis was done with the enhanced chemiluminescence (ECL) kit from Amersham Pharmacia. Cell lysates were prepared from primary chondrocytes as described (15). SOX9 antibodies were described and used at a 1:1000 dilution (16). β-actin antibodies (Sigma) were diluted 1:1000.

Results

***Sox9* Heterozygotes Die Shortly After Birth.** To determine the role of *Sox9*, we previously had generated *Sox9* heterozygous ($Sox9^{+/-}$) and homozygous ($Sox9^{-/-}$) mutant ES cells by homologous recombination (3). In the mutant allele of *Sox9*, a 300-bp deletion of part of exon 1, including the translation initiation site and a portion of the sequence coding for the HMG domain, was replaced with an IRES-*lacZ*-PGK-*neo*-bpA cassette. No *Sox9* transcripts were detected in E10.5 embryos derived exclusively from *Sox9* homozygous mutant ES cells, indicating that the mutant allele we generated was null for *Sox9* (D.J.W., W.B., B.deC., and R.R.B., unpublished data). Germline transmission of the *Sox9 lacZ-neo* allele was obtained for two targeted clones. $Sox9^{+/-}$ mice derived from these clones exhibited the same mutant phenotype. Chondrocytes from $Sox9^{+/-}$ newborn mice showed a significant reduction in the expression of both *Sox9* RNA and protein compared with wild-type chondrocytes (Fig. 1).

All $Sox9^{+/-}$ mutants generated by crossing chimeric male

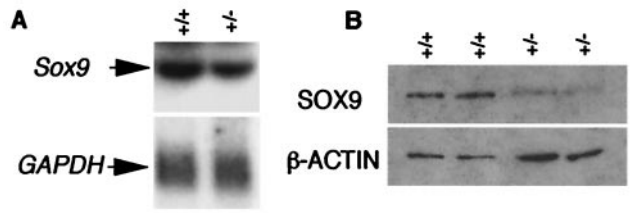

Fig. 1. Expression of *Sox9* in primary chondrocytes isolated from wild-type (+/+) and heterozygous (+/−) neonates. (*A*) Northern analysis. Ten micrograms of total RNA was hybridized with a *Sox9* probe from the deleted region. The same membrane then was hybridized with *GAPDH* as an RNA-loading control for the quantity of RNA. (*B*) Western blotting with SOX9 antibody. β-actin antibody (Sigma) was used on the same membrane as a protein-loading control.

founders and CD-1 females died within the first 20 h after birth. Both male and female $Sox9^{+/-}$ mutants were obtained. The mutants displayed a gasping respiration and accumulated air in their stomachs and intestines. The newborn mutants were usually more slender but had an overall length that was similar to that of their wild-type littermates (Fig. 2 *A* and *B*). A shortened lower jaw and frequently a crooked tail were observed in the mutant neonates.

$Sox9^{+/-}$ mutants had a bilateral cleft of the secondary palate at birth. Histological analysis showed that the secondary palate was not formed in *Sox9* heterozygotes, although the two palatal shelves were present (Fig. 2 *C* and *D*). The mutants also had a bifurcated tongue, but tooth development was not affected. Both upper and lower incisors and molars seemed normal. Testes from *Sox9* heterozygotes of different genetic backgrounds were examined. At E14.5, testes from heterozygotes of 129SvEv/C57B6 and 129SvEv/Swiss mixed backgrounds and those from a 129SvEv inbred background were histologically normal (Fig. 2 *E* and *F* and data not shown). Expression of the *Sox9 lacZ-neo* mutant allele in heterozygous mutants, detected by β-galactosidase activity, recapitulated the normal expression pattern of *Sox9* (4, 5). The expression pattern of the *Sox9* mutant allele also indicated that there was no transformation of skeletal structures, implying that *Sox9* haploinsufficiency does not affect patterning of skeletal elements.

Skeletal Malformations in *Sox9* Heterozygotes. Alcian blue and Alizarin red S staining of $Sox9^{+/-}$ E18.5 and newborn mutants revealed hypoplasia of nearly all skeletal elements derived by endochondral ossification. All $Sox9^{+/-}$ mutants showed different degrees of bilateral and anterior bending of long bones including the ulnae, radii, and tibiae, with the most severe bending always observed in the ulnae (Fig. 2 *G* and *H*). The bending of the radii occurred in the middle of the bone shaft, whereas the acute angulation of the ulnae was more anterior in the bone shaft. The bending was symmetrical, but the severity of bending varied among individuals from slight bowing to obvious angulation. In $Sox9^{+/-}$ E18.5 embryos, the scapulae were hypoplastic (Fig. 2*H*). The pelvic bones of $Sox9^{+/-}$ neonates were smaller and the ilium, ischium, and pubic bones were thinner (Fig. 2 *I* and *J*). In severely affected animals, the ilium was angulated and the pubic bone was bent (Fig. 2*J*). In all heterozygotes examined, scapulae and pelvic bones were affected symmetrically on each side of the midline.

In $Sox9^{+/-}$ neonates, a small rib cage was evident that was caused in large part by a shorter sternum (Fig. 2 *K* and *L*). The sternebrae were also thinner and not as regular as those in wild-type controls. The manubrium sternum of $Sox9^{+/-}$ mutants was missing or exhibited anterior bending. The xiphoid process

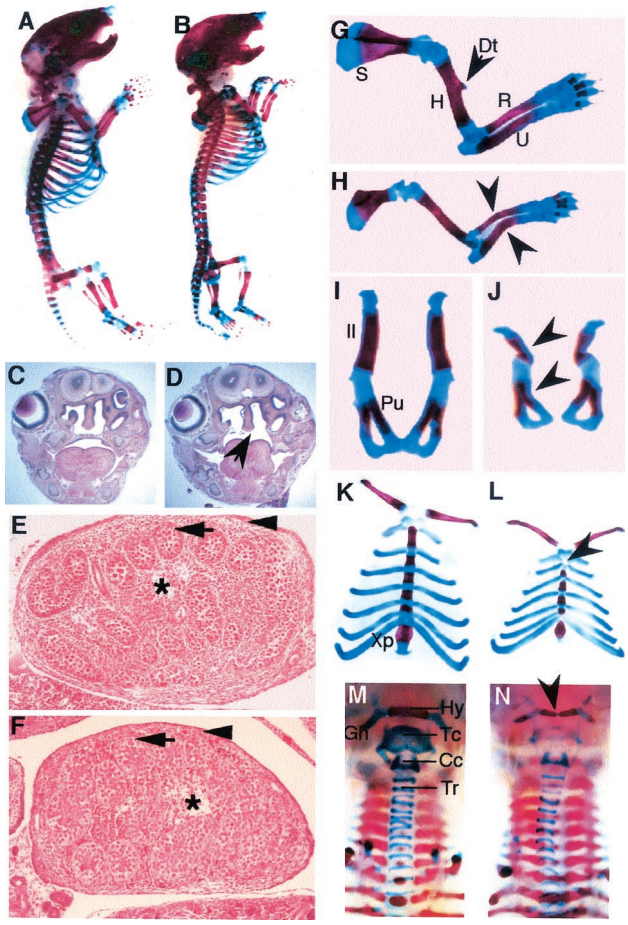

Fig. 2. Skeletal malformations in *Sox9*$^{+/-}$ embryos. (*A* and *B*) Lateral view of the skeletal preparation of wild-type (*A*) and heterozygous (*B*) newborns. (*C* and *D*) Hematoxylin/eosin-stained coronal sections of the heads at the level of molars of E18.5 wild-type (*C*) and *Sox9*$^{+/-}$ (*D*) embryos. The arrow indicates the cleft palate in the mutants. (*E* and *F*) Transverse sections through testes of E14.5 *Sox9*$^{+/-}$ embryos. (*E*) Wild-type testis (Swiss) showed seminiferous cords (arrow) enclosing the germ cells. Fetal Leydig cells comprise the interstitium (asterisk) between the seminiferous cords, and a tunica albuginea (arrowhead) surrounds the testis. (*F*) *Sox9*$^{+/-}$ testis (129SvEv/C57B6) was histologically normal. (*G–N*) Dissected skeletal elements of wild-type controls (*G*, *I*, *K*, and *M*) and *Sox9*$^{+/-}$ mutants (*H*, *J*, *L*, and *N*). (*G* and *H*) E18.5 forelimbs. The deltoid tuberosity (Dt) of the humerus was missing in the mutants. Arrowheads indicate the bending of the radius and ulna. (*I* and *J*) E18.5 pelvic bones. Arrowheads indicate a bending ilium and pubic bone. (*K* and *L*) E18.5 rib cages. Arrowhead indicates a missing manubrium sterna. (*M* and *N*) Newborn trachea. Arrowhead indicates the bending of the hyoid bone in the *Sox9*$^{+/-}$ mutants. S, scapula; H, humerus; R, radius; U, ulna; Il, ilium; Pu, pubic; Xp, xiphoid process; Hy, hyoid bone; Tc, thyroid cartilage; Cc, cricoid cartilage; Tr, tracheal rings.

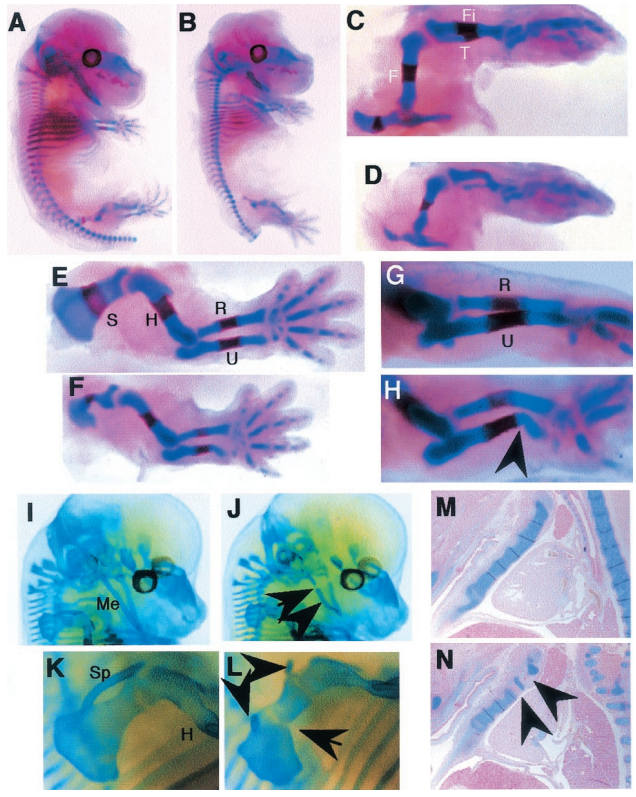

Fig. 3. Abnormalities in the cartilaginous elements in *Sox9*$^{+/-}$ embryos at E14.5. (*A–H*) Skeletal preparation of wild-type (*A*, *C–E*, and *G*) and *Sox9*$^{+/-}$ embryos (*B–D*, *F*, and *H*). Arrowhead in *H* indicates that the bending site of the ulna was outside the ossification center. (*I–L*) Cartilage staining of wild-type (*I* and *K*) and *Sox9*$^{+/-}$ (*J* and *L*) embryos. Meckel's cartilage was interrupted (arrow) and bowing (arrowhead) in the mutants (*J*). (*K* and *L*) Scapulae. Arrowheads indicate a missing spine and arrow indicates the hypoplastic blade in the mutants. (*M* and *N*) Sections of E15.5 sternum of wild-type (*M*) and *Sox9*$^{+/-}$ embryos (*N*). The cartilage primordia of the sternum were malformed in the mutants as indicated by arrows. Me, Meckel's cartilage; S, scapula; Sp, spine of scapula; H, humerus; R, radius; U, ulna; F, femur; Fi, fibula; T, tibia.

was affected also, with a much smaller xiphoid cartilage (Fig. 2 *K* and *L*).

In *Sox9*$^{+/-}$ mutants, the hyoid bone, laryngeal cartilage, and tracheal rings of the respiratory tract were thinner and stained more weakly by Alcian blue (Fig. 2 *M* and *N*). The body of the hyoid bone was bent in the center with the central part of the hyoid bone missing in severely affected mutants. The malformations of the trachea in the heterozygotes indicated that the loss of one functional *Sox9* allele also affected permanent cartilage elements.

Abnormalities in Cartilage Primordia. To understand further the skeletal defects of *Sox9*$^{+/-}$ mutants, we examined the developmental course of the skeletal malformations. Essentially all endochondral skeletal elements of E14.5 heterozygous mutant embryos were smaller and thinner than those in wild-type controls (Fig. 3 *A–F*). At the base of the skull, the cartilage precursor of the occipital bone was much smaller and stained less intensely with Alcian blue. Meckel's cartilage was interrupted and bent toward the body midline, appearing much shorter because of the bending (Fig. 3 *I* and *J*). This impaired Meckel's cartilage accounts for the smaller mandible observed in mutant neonates. In E14.5 *Sox9*$^{+/-}$ embryos, the cartilage precursor of scapulae were severely hypoplastic (Fig. 3 *E* and *F* and *K* and *L*); the blades of the heterozygous scapulae consisted of two parts that were not connected completely. Moreover, only the two ends of the spines were present in mutants, with the major central part missing (Fig. 3 *K* and *L*). Prominent bending and angulation of the ulnae, radii, and tibiae were present (Fig. 3 *C–H*). The bending site was located outside of the mineralization region, indicating that the bending of long bones was caused by bending of cartilaginous bone primordia (Fig. 3 *G* and *H*).

In E15.5 *Sox9* heterozygotes, formation of the sternal bars that connect the costal cartilages at the ventral ends of the ribs was affected. Normally at E15.5, the sternal bars are well formed and are able to be stained by Alcian blue (Fig. 3*M*; ref. 17). However, in *Sox9*$^{+/-}$ mutants, the cartilaginous sternum was shorter with some cartilaginous elements that had not yet formed, leaving an Alcian blue-unstained space between sternal bars (Fig. 3*N*). The

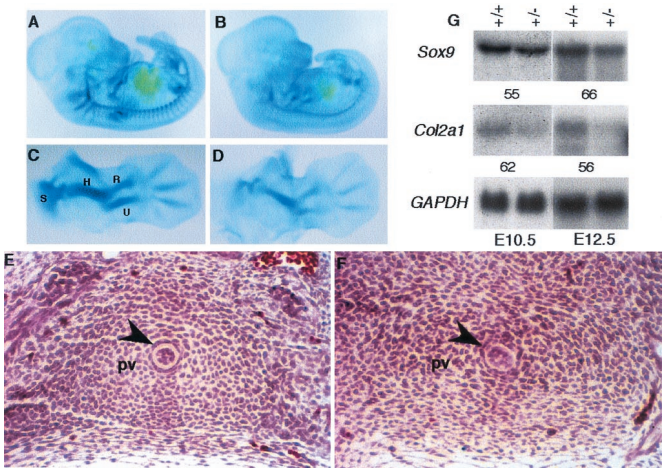

Fig. 4. Alcian blue staining of wild-type (*A* and *C*) and *Sox9*$^{+/-}$ (*B* and *D*) embryos at E12.5. (*A* and *B*) Whole embryos. (*C* and *D*) Forelimbs. (*E* and *F*) Hematoxylin/eosin staining of transverse sections through equivalent thoracic regions. Cells in the sclerotome surrounding the notochord (arrowhead) appeared like mesenchymal cells in the *Sox9*$^{+/-}$ mutants (*F*), but were typical cobblestone-like prechondrocytic cells in wild-type controls (*E*). (*G*) Northern analysis with total RNA from wild-type (+/+) and *Sox9*$^{+/-}$ mutant (+/−) embryos at E10.5 and E12.5. The expression levels of *Sox9* and *Col2a1* were measured by densitometry in a PhosphorImager (Molecular Dynamics) and the percent expression levels of the mutant relative to wild type are shown. S, scapula; H, humerus; R, radius; U, ulna; F, femur; Fi, fibula; T, tibia; Pv, prevertebrae.

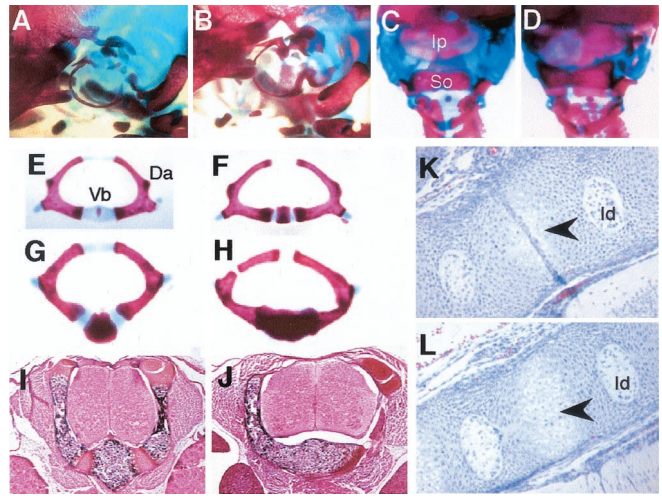

Fig. 5. Premature mineralization in the *Sox9*$^{+/-}$ mutants. (*A–H*) Skeletal preparation of wild-type (*A*, *C*, *E*, and *G*) and *Sox9*$^{+/-}$ (*B*, *D*, *F*, and *H*) newborns. (*A* and *B*) Middle ears. (*C* and *D*) Dorsal view of the skull. (*E* and *F*) Seventh cervical vertebrae. (*G* and *H*) Third thoracic vertebrae. (*I* and *J*) Von Kossa staining of sections of fifth thoracic vertebrae. The cartilaginous regions between the vertebral body and the pedicles of dorsal arches in wild-type control (*I*) were mineralized in E18.5 *Sox9*$^{+/-}$ mutants (*J*). (*K* and *L*) Hematoxylin/eosin staining of sections of equivalent caudal vertebrae from E15.5 wild-type (*K*) and *Sox9*$^{+/-}$ (*L*) embryos. The area of hypertrophic chondrocytes are indicated by arrowheads. Ip, interparietal bone; So, supraoccipital bone; Vb, vertebral body; Da, dorsal arch; Id, intervertebral discs.

smaller and irregular sternal bars present at later stages were presumably a result of delayed development of these skeletal elements.

We concluded that the skeletal malformations in the *Sox9*$^{+/-}$ mutants were caused by defective cartilage skeletal precursors.

Impaired Development of Precartilaginous Mesenchymes. In E12.5 *Sox9*$^{+/-}$ mutants, all precartilaginous skeletal elements visualized by using Alcian blue staining exhibited reduced staining intensity and were smaller than in wild-type controls (Fig. 4 *A–D*). For example, in E12.5 heterozygotes, the cartilage primordia of scapula consisted of two small pieces instead of a single intact element, as is normally found in wild-type embryos (Fig. 4 *C* and *D*). Histological analysis of E12.5 *Sox9*$^{+/-}$ and wild-type embryos showed that in the heterozygotes, the chondroprogenitors surrounding the notochord in the vertebral primordia were still elongated mesenchymal cells with little matrix around the cells (Fig. 4*F*). In contrast, in equivalent vertebral primordia of wild-type embryos, these cells were already typical cobblestone-like chondrogenic cells surrounded by abundant matrix (Fig. 4*E*). These results suggest that despite the fact that the domains of expression of *Sox9* were unchanged in *Sox9*$^{+/-}$ mutant embryos, the development of cartilage primordia was delayed and was of smaller size.

Expression levels of *Sox9* and *Col2a1*, examined by Northern blot, were decreased when RNAs from whole E10.5 and E12.5 embryos were used (Fig. 4*G*). Overall, our results indicate that correct development of cartilage primordia seems to be delayed in heterozygotes because of dosage insufficiency of *Sox9*.

Premature Skeletal Mineralization in *Sox9*$^{+/-}$ Mice. Mineralization of skeletal elements is an ordered and precisely controlled process. In *Sox9*$^{+/-}$ neonates, premature mineralization occurred in many skeletal elements including craniofacial bones and vertebrae (Fig. 5). The heterozygotes had a similar-sized skull but generally showed more extended calcified areas, stained by Alizarin red, and fewer cartilaginous regions, stained by Alcian blue (Fig. 5 *A–D*). In *Sox9*$^{+/-}$ mutants, advanced mineralization also was observed in bony ossicles of the middle ear (Fig. 5 *A* and *B*). Ossification centers of the interparietal and supraoccipital bones were expanded also (Fig. 5 *C* and *D*).

The vertebrae and ribs are derived from sclerotomes. Advanced mineralization was found in the vertebrae throughout the vertebral columns of *Sox9*$^{+/-}$ neonates (Fig. 5 *E–J*). The ossification centers of the cervical vertebrae were larger or appeared earlier than those of the corresponding vertebrae in wild-type controls. In the thoracic regions, ossification in each dorsal-arch unit already extended ventrally to fuse with the ossification centers of the vertebral bodies (Fig. 5 *G–J*). Dissection of the vertebral axis revealed that the shape of the vertebrae was normal although occasionally part of the dorsal arch was missing (Fig. 5*H*); cartilaginous elements in the dorsal parts of the vertebrae stained more weakly with Alcian blue or were simply missing (Fig. 5 *F* and *H*). Consistent with the premature mineralization of vertebrae in neonatal *Sox9*$^{+/-}$ mutants, sections through equivalent caudal vertebrae of E15.5 embryos indicated that the process of differentiation of hypertrophic chondrocytes was advanced more in *Sox9*$^{+/-}$ mutants than in wild-type littermates (Fig. 5 *K* and *L*).

The ossification centers of the talus and the calcaneum in the hindlimbs were enlarged in the heterozygous mutants, and the secondary ossification center at the proximal end of scapulae was formed earlier in the heterozygotes also (data not shown). Ossification occurred prematurely in both greater horns of the hyoid bone, whereas it normally occurs only postnatally (Fig. 2 *M* and *N*).

We also analyzed the epiphyseal growth plates of the tibiae of *Sox9*$^{+/-}$ neonates and E18.5 embryos by histological analysis and *in situ* hybridization (Fig. 6). All components of the growth plates were present in *Sox9*$^{+/-}$ mutants (Fig. 6 *A* and *B*); more specifically, the zones of resting and proliferating chondrocytes in *Sox9*$^{+/-}$ mutants appeared normal. Von Kossa staining showed that the calcification of the terminal hypertrophic chondrocytes was normal (data not shown). However, histological

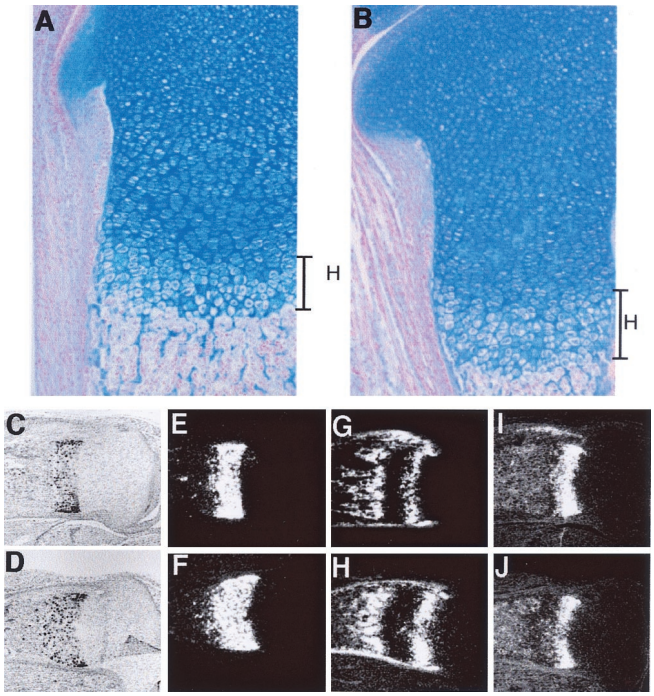

Fig. 6. Enlarged hypertrophic zone in *Sox9*$^{+/-}$ epiphyseal growth plate of the proximal tibia. (*A* and *B*) Alcian blue staining of the epiphyseal growth plates of wild-type (*A*) and *Sox9*$^{+/-}$ (*B*) embryos at E18.5. (*C–J*) RNA *in situ* hybridization analysis of the expression of *Col10a1* (*E* and *F*), parathyroid hormone receptor (*PTHrP-R*; *G* and *H*), and Indian hedgehog (*Ihh*; *I* and *J*) in the tibia epiphyseal growth plates of wild-type (*C*, *E*, *G*, and *I*) and *Sox9*$^{+/-}$ (*D*, *F*, *H*, and *J*) neonates. (*C* and *D*) Bright field. H, hypertrophic zone.

analysis of the growth plate at E18.5 showed that the hypertrophic zone in the *Sox9* heterozygotes was enlarged (Fig. 6 *A* and *B*). *In situ* hybridization indicated that type X collagen RNA was expressed in a wider region in growth plates of *Sox9*$^{+/-}$ neonates (Fig. 6 *E* and *F*). No major changes were seen in the pattern of expression of parathyroid hormone receptor and of Indian hedgehog (Fig. 6 *G–J*). The enlargement of the hypertrophic zones of the epiphyseal growth plates in the absence of one functional allele suggested that *Sox9* regulates the rate of hypertrophic chondrocyte differentiation.

Discussion

Hypoplastic Cartilage Primordia Are Caused by *Sox9* Haploinsufficiency. Heterozygous *Sox9* mutant mice are characterized by hypoplasia of all bones formed by endochondral ossification of all cartilages. In E14.5 *Sox9*$^{+/-}$ mutant embryos, all cartilage skeletal elements were already thinner or smaller. There were, however, no obvious patterning defects, suggesting that *Sox9* haploinsufficiency does not influence skeletal-pattern formation. The bending observed in several hypoplastic cartilaginous bone precursors may be caused by fetal muscle contraction.

In E12.5 wild-type embryos, cartilages begin to form from mesenchymal condensations, whereas in distal parts of limbs mesenchymal condensations form from committed cells. At this stage, all cartilages and cartilage primordia visualized by using Alcian blue staining were hypoplastic. In addition, the chondroblasts surrounding the notochord in *Sox9*$^{+/-}$ embryos still had the aspect of mesenchymal cells, whereas at equivalent locations in wild-type embryos these cells were more chondrocytic. Consistent with this finding, we found lower levels of *Col2a1* RNA in whole E12.5 and E10.5 *Sox9*$^{+/-}$ mutant embryos compared with wild-type littermates. A reduction of *Col2a1* RNA levels was observed also by *in situ* hybridization of *Col2a1* at E10.5 and E11.5 (data not shown). The hypoplastic cartilages and cartilage primordia in *Sox9*$^{+/-}$ mutants could be because of a reduced proliferation rate of cells in mesenchymal condensations and in forming cartilages. However, when cells present in E12.5 vertebrae were labeled by BrdUrd or examined for proliferating cell nuclear antigens, they showed the same density of proliferating cells in *Sox9*$^{+/-}$ and wild-type embryos, indicating that haploinsufficiency of *Sox9* did not affect the rate of cell proliferation (data not shown). Given that *Sox9* is required for chondrogenic mesenchymal condensations, we propose that the hypoplastic cartilages are caused by defective mesenchymal condensations in heterozygous animals, perhaps because fewer cells are recruited to the mesenchymal condensations. A study using simulations of stochastic gene expression has suggested that inactivation of a single allele of a gene in diploid organisms could decrease the probability of expression of this gene, and that initiation of gene expression could be delayed in the absence of one functional allele (18). It is possible that some *Sox9*-dependent genes that are needed for precartilaginous mesenchymal condensations are not expressed at sufficient levels in the mutants. Correct expression of these genes would need a threshold level of *Sox9* that would be reached less frequently in heterozygous mutants than in wild-type embryos. It should be noted that the K_d for SOX9 binding to DNA is in the nanomolar range (19), in contrast to the K_d of many other transcription factors that are in the picomolar range. It is therefore conceivable that the absolute concentration of SOX9 is near the K_d value in wild-type individuals, thus a 50% reduction in *Sox9* would affect transcription of at least some *Sox9*-dependent genes.

***Sox9* Regulates the Rate of Hypertrophic Chondrocyte Differentiation.** Premature mineralization was observed in many skeletal elements of *Sox9*$^{+/-}$ mutant mice. Because expression of *Sox9* RNA and protein is shut off completely in the hypertrophic zone, this premature mineralization is most likely a consequence of the haploinsufficiency existing in *Sox9*-expressing cells that are progenitors of the hypertrophic chondrocytes.

Despite the hypoplasia of cartilage primordia, the different cellular components of the growth-plate cartilage were present and their organization appeared normal. Thus the chondrocytes were responding normally to signals that result in the proper cellular organization of the growth plate. However, comparison of the length of different zones in these growth plates showed that the hypertrophic zone was expanded in the *Sox9*$^{+/-}$ mutants. We propose that *Sox9* has a role in regulating the rate of chondrocyte differentiation into hypertrophy, and that *Sox9*

Table 1. Comparison of the skeletal abnormalities in patients with CD and *Sox9*$^{+/-}$ mice

Features	Patients with CD	*Sox9* mutant mice
Early death	+	+
Respiratory distress	+	+
Cleft palate	+	+
Tracheobronchial hypoplasia	+	+
Small thoracic cage	+	+
Micrognathia	+	+
Bowing of long bones	+	+
Bowed tibiae	+	+
Bowed femora	+	−
Bowed ulnae or radii	−	+
Bowed manubrium sternae	−	+
Hypoplastic scapulae	+	+
Deformed pelvis and spine	+	+
Missing pair of ribs	+	−

might function in maintaining the chondrocyte phenotype by inhibiting hypertrophic chondrocyte differentiation. *Sox9* haploinsufficiency would result in accelerated hypertrophic differentiation and subsequently in premature mineralization. The normal inhibition of hypertrophic chondrocyte differentiation may require a level of *Sox9* activity that is not attained in the prehypertrophic zone of the $Sox9^{+/-}$ mutants. This view is supported by recent experiments suggesting that *Sox9* might be a physiological target of parathyroid hormone (PTHrP) signaling, and might mediate at least in part the effects of PTHrP in maintaining cells as nonhypertrophic cells (20). Altogether these experiments favor the view that the function of *Sox9* in chondrogenesis extends beyond the step of mesenchymal condensations.

Analogies Between Skeletal Dysmorphologies of $Sox9^{+/-}$ Mice and Patients with CD. Many of the skeletal defects observed in $Sox9^{+/-}$ mice phenocopy those of the human disease CD as shown in Table 1. Despite many striking similarities in the skeletal defects of $Sox9^{+/-}$ mice and patients with CD, some differences exist nonetheless. In patients with CD, bending of bones usually is observed in tibiae and femora, but occurs very rarely in the upper limbs (9, 10). In contrast, in $Sox9^{+/-}$ mutant mice, skeletal elements in both forelimbs and hindlimbs, including ulnae, radii, and tibiae, exhibited bending, whereas the proximal bones were hypoplastic but did not show bending. These discrepancies could be the result of relative skeletal differences in the overall shape of specific cartilage primordia between humans and mice.

The skeletal defects of patients with CD show a wide variation among affected individuals (10). In mice, the phenotypic manifestations of the heterozygous *Sox9* mutations were influenced strongly by their genetic background. In $Sox9^{+/-}$ mutant mice on the 129SvEv inbred background, the skeletal defects were more severe. The genetic background effects might be caused by other loci that encode proteins that cooperate with *Sox9*. Because *L-Sox5* and *Sox6* have been shown to cooperate with *Sox9* in activating the *Col2a1* and *aggrecan* (21), the expression of *L-Sox5* and *Sox6* could conceivably influence the effect of a given *Sox9* mutation.

Because several lines of evidence indicate that our targeted mutation is a null allele (3), we can exclude the creation of a dominant-negative-acting SOX9 mutant polypeptide. Thus, our data demonstrate that the function of *Sox9* is dosage-dependent, and that the reduction in the expression level of *Sox9* affects all endochondral and cartilage skeletal elements.

In summary, analysis of $Sox9^{+/-}$ mutants indicated that two steps in the pathway of chondrocyte differentiation are sensitive to *Sox9* dosage. *Sox9* haploinsufficiency results in defective cartilage primordia, which in turn are the causes for the hypoplasia and the eventual bending of the cartilaginous and endochondral skeletal elements. The premature mineralization of many skeletal elements indicates that another step preceding the formation of hypertrophic chondrocytes in the growth plate is also sensitive to *Sox9* dosage.

We thank Gerald Pinero and Heidi Ebspaecher for histological assistance. We also thank R. Johnson for the Indian hedgehog probe and M. Kronenberg for the parathyroid hormone receptor probe. This work was funded by National Institutes of Health Grants P01 AR42919 (to B.deC. and R.B.) and R01 HD30284 (to R.B.). DNA sequencing was supported by National Institutes of Health Grant CA16672.

1. Tacchetti, C., Tracella, S., Dozin, B., Quarto, R., Robino, G. & Cancedda, R. (1992) *Exp. Cell Res.* **200,** 26–33.
2. Cancedda, R., Descalzi Cancedda, F. & Castagnola, P. (1995) *Int. Rev. Cytol.* **159,** 265–358.
3. Bi, W., Deng, J. M., Zhang, Z., Behringer, R. R. & de Crombrugghe, B. (1999) *Nat. Genet.* **22,** 85–89.
4. Wright, E., Hargrave, M. R., Christiansen, J., Cooper, L., Kun, J., Evans, T., Gangadharan, U., Greenfield, A. & Koopman, P. (1995) *Nat. Genet.* **9,** 15–20.
5. Zhao, Q., Eberspaecher, H., Lefebvre, V. & de Crombrugghe, B. (1997) *Dev. Dyn.* **209,** 377–386.
6. Wagner, T., Wirth, J., Meyer, J., Zabel, B., Held, M., Zimmer, J., Pasantes, J., Bricarelli, F. D., Keutel, J., Hustert, E., *et al.* (1994) *Cell* **79,** 1111–1120.
7. Ng, L.-J., Wheatley, S., Muscat, G. E. O., Conway-Campbell, J., Bowles, J., Wright, E., Bell, D. M., Tam, P. P. L., Cheah, K. S. E. & Koopman, P. (1997) *Dev. Biol.* **183,** 108–121.
8. Foster, J. W., Dominguez-Steglich, M. A., Guioli, S., Kwok, C., Weller, P. A., Stevanovic, M., Weissenbach, J., Mansour, S., Yong, I. D., Goodfellow, P. N., *et al.* (1994) *Nature (London)* **372,** 525–530.
9. Houston, C. S., Opitz, J. M., Spranger, J. W., MacPherson, R. I., Reed, M. H., Gilbert, E. F., Herrmann, J. & Schinzel, A. (1983) *Am. J. Med. Genet.* **15,** 3–28.
10. Mansour, S., Hall, C. M., Pembrey, M. E. & Young, I. D. (1995) *J. Med. Genet.* **32,** 415–420.
11. Mcleod, M. J. (1980) *Teratology* **22,** 299–301.
12. Ojeda, J. L., Barbosa, E. & Bosque, P. G. (1970) *Stain Technol.* **45,** 137–138.
13. Mertin, S., McDowall, S. G. & Harley, V. R. (1999) *Nucleic Acids Res.* **27,** 1359–1364.
14. Metsaranta, M., Toman, D., de Crombrugghe, B. & Vuorio, E. (1991) *Biochim. Biophys. Acta* **1089,** 241–243.
15. Coustry, F., Maity, S. N. & de Crombrugghe, B. (1995) *J. Biol. Chem.* **270,** 468–475.
16. Lefebvre, V., Huang, W., Harley, V. R., Goodfellow, P. N. & de Crombrugghe, B. (1997) *Mol. Cell. Biol.* **17,** 2336–2346.
17. Kaufman, M. H. & Bard, J. B. L. (1999) in *The Anatomical Basis of Mouse Development* (Academic, London), pp. 58–59.
18. Cook, D. L., Gerber, A. N. & Tapscott, S. J. (1998) *Proc. Natl. Acad. Sci. USA* **95,** 15641–15646.
19. Goldberg, H., Helaakoski, T., Garrett, L. A., Karsenty, G., Pellegrino, A., Lozano, G., Maity, S. N. & de Crombrugghe, B. (1992) *J. Biol. Chem.* **267,** 19622–19630.
20. Huang, W., Chung, U., Kronenberg, M. H. & Benoit de Crombrugghe. (2001) *Proc. Natl. Acad. Sci. USA* **98,** 160–165. (First Published December 19, 2000; 10.1073/pnas.011393998)
21. Lefebvre, V., Li, P. & de Crombrugghe, B. (1998) *EMBO J.* **17,** 5718–5733.